Variability of At-Satellite Surface Reflectance from Landsat TM and NOAA AVHRR in Death Valley National Monument

Thomas D. Frank, Scott A. Tweddale, and David E. Knapp

Abstract

The spatial and temporal variability of surface reflectance has been recognized as a good indicator of the condition of arid and semi-arid landscapes. However, radiometric, atmospheric, and topographic factors all affect the measurement of surface reflectance from satellites such as Landsat Thematic Mapper (TM) and NOAA Advanced Very High Resolution Radiometer (AVHRR). The effect of deriving surface reflectance from satellites with different spectral wavebands is an important issue if regional or global scale monitoring of arid landscapes is to be successful with satellite observations. Radiometric, atmospheric, and topographic influences on surface reflectance were examined in this study of surficial geologic units in Death Valley National Monument with coincident TM, AVHRR, and in situ *measurements of surface reflectance. The results of this study indicated that spectral wavelength affected the estimate of surface reflectance more than any other factor. The short-wave surface reflectance waveband covering red through near-infrared provided both the closest agreement between satellites, and between satellites and* in situ *measurements. Topographic effects on surface reflectance were apparent in the mountains surrounding Death Valley National Monument, but for the relatively gentle slopes along the alluvial fans adjacent to the valley floor, significant topographic effects were not observed.*

Introduction

The global distribution of deserts and estimates of their condition are widely known (Dregne, 1981), and international efforts have been focused to identify the nature and pattern of degradational processes and to develop measures to reduce land degradation (Gerasimov, 1986). Satellite observations have been used in some of these efforts to monitor the condition of desert landscapes because large regions, global scale phenomena, and long-term temporal change have been the focus of attention (e.g., Justice *et al.*, 1989; Graetz and Pech, 1988; Pech *et al.*, 1986; Smith *et al.*, 1990a; Smith *et al.*, 1990b). Then the spatial and temporal variability of surface reflectance, defined as the ratio of the amount of electromagnetic energy reflected from the surface to the amount of radiation incident upon the surface (Sellers, 1965), has been promoted as an expression of the condition of landscapes, or as an indicator of change in landscapes (e.g., Robinove *et al.*, 1981; Frank, 1984; Nelson *et al.*, 1987; Nunez *et al.*, 1987; Otterman and Tucker, 1985). While considerabe attention has been given to assess the spectral reflectance from vegetation and soils in arid and semiarid environments (e.g., Charney *et al.*, 1977; Graetz and Gentle, 1982; McDaniel and Haas, 1982; Gillespie *et al.*, 1984; Davis *et al.*, 1987; Petersen *et al.*, 1987), relatively little attention has been given to assess the temporal and spatial variability of satellite-based surface reflectance when the estimates are made from different satellites. Comparisons between satellites will be necessary to monitor degradation in desert ecosystems because of the diverse spatial and temporal scales at which degradation occurs in arid and semi-arid landscapes. Therefore, surface reflectance models that are applicable to all times and locations, and that are independent of sensor, atmospheric, and topographic considerations, are needed to assess land degradation.

The objective of this paper has been to evaluate the sources of variation in at-satellite surface reflectance along a brightness gradient associated with surficial geologic units in Death Valley National Monument in the western United States. Seven geologic units have been observed with coincident Landsat Thematic Mapper (TM), NOAA Advanced Very High Resolution Radiometer (AVHRR), and *in situ* spectral reflectance measurements. The study was designed to assess the effects of spectral resolution, the additive effects of atmospheric scattering, the depletionary effects of the optical air mass, and the topographic effects of surface slope and aspect on reflectance in the highly reflective desert landscape typically found in the deserts of the western United States. The specific goal of this study has been to determine whether comparable surface reflectance measurements can be derived from the high resolution and low resolution satellite data, to assess whether these values agree with a limited number of *in situ* measurements of reflectance, and to determine which spectral wavebands would be most beneficial to monitor degradation in arid and semiarid environments.

Radiometric Calibration of Satellite Data

Surface reflectance can be derived from satellite measurements if the direct, diffuse, and reflected components of irra-

T. D. Frank is with the Department of Geography, University of Illinois, Urbana, IL 61801.

S. A. Tweddale, Geographic Information Systems Laboratory, University of Illinois, Urbana, IL 61801.

D. E. Knapp is with Hughes STX, Inc., Lanham, MD 20706.

Photogrammetric Engineering & Remote Sensing, Vol. 60, No. 10, October 1994, pp. 1259–1266.

0099-1112/94/6010-1259$3.00/0
© 1994 American Society for Photogrammetry and Remote Sensing

diance and the path radiance and transmittance characteristics (τ) of the atmosphere (Kaufman, 1989) are known (Equation 1): i.e.,

$$\rho_s = \frac{\pi(Ls_\lambda - (Lo_\lambda + Ld1_\lambda + Ld2_\lambda))d^2}{\tau_\lambda^{\sec\theta} E_\lambda \cos\theta + \text{sky}_\lambda} \quad (1)$$

where

ρ_s = at-satellite, in-band surface reflectance estimate for a specified waveband interval;
L_s is the attenuated signal; the radiance of light in mW cm^2 μm^1 sr^1 transmitted directly downward through the atmosphere, reflected from the surface, and directly transmitted through the atmosphere to the sensor;
L_o is the path radiance; the radiance of light scattered from the direct sunbeam by the atmosphere into the sensor's field of view without being reflected from the surface;
L_{d1} is the radiance of light scattered by the atmosphere before reaching the surface, reflected by the surface, and directly transmitted through the atmosphere to the sensor;
L_{d2} is the radiance of light reflected by the surface and then transmitted to the sensor with at least one scattering in the atmosphere;
d = Earth-sun distance in astronomical units;
E = exoatmospheric spectral irradiance at top of the atmosphere in mW cm^2 μm^1 for a specified waveband interval;
θ = the solar zenith angle;
τ_λ = atmospheric transmittance coefficient for the specified waveband interval;
sec θ = correction for the optical air mass; and
sky_λ = the diffuse component of irradiance.

Surface reflectance is affected by the type and distribution of terrestrial components in the landscape, while the path radiance (L_o) is affected by the amount and distribution of gas molecules and solid particles in the atmosphere (e.g., Rayleigh and Mie scattering). Both surface reflectance and path radiance vary temporally and spatially, but the path radiance is particularly difficult to model because atmospheric conditions change so abruptly.

The relative contribution of direct radiation at the surface is a function of the solar zenith angle (θ), atmospheric transmittance characteristics of specified wavebands (τ), the Earth-sun distance (d), and the optical thickness of the atmosphere (Slater, 1983). Diffuse solar radiation is a function of atmospheric scattering in much the same manner as path radiance. The reflected component of irradiance results from the reflection of solar radiation from surrounding features in the landscape, such as large mountains, and from the lower parts of the atmosphere when the terrestrial surfaces are very bright. Upwelling reflected radiation from the surface into the base of the atmosphere can be scattered back down to the surface as an additional source of irradiance in arid and semiarid landscapes, particularly when the surface albedo is greater than 0.22 (Chen and Ohring, 1984). Scattered upwelling radiation is affected by the transmission characteristics of the lower atmosphere, but for Lambertian surfaces, this component is independent of the solar zenith angle (Chahine *et al.*, 1983).

Topography affects spectral radiance observed by satellite sensors because reflectance is generally darker on slopes facing away from the sun, and lighter on slopes facing into the sun. The relationship between direct solar beam and the landscape surface depends on the position of the sun at a given time of day on a given day of the year, the latitude and longitude of the landscape unit, and the slope and aspect of the terrain at that location. The topographic affect on reflectance has been described by Dozier and Strahler (1983), Kawata *et al.*, (1988), and Civco (1989). Cosine solar zenith angle to a sloping surface $\cos\theta_s$ is modeled after the cosine law of spherical geometry, where

$$\cos\theta_s = f(\phi,\delta,\psi,\alpha,\beta) \quad (2)$$

where

ϕ = latitude,
δ = solar declination,
ψ = hour angle,
α = ground aspect, and
β = ground slope

Then (after Garnier and Ohmura , 1968):

$$\cos\theta_s = (\cos\phi\cos\psi\cos\beta - \sin\psi\sin\alpha\sin\beta - \sin\phi\cos\psi\cos\alpha\sin\beta)\cos\delta + (\cos\phi\cos\alpha\sin\beta + \sin\phi\cos\beta)\sin\delta \quad (3)$$

Then $\cos\theta_s$ can be substituted in Equation 1 to derive at-satellite topographically corrected reflectance (ρ_t). Note that atmospheric transmittance is adjusted as a power function of solar zenith angle to a horizontal surface while solar exoatmospheric irradiance is adjusted as a function of the solar zenith angle to the topographic surface.

Study Site

Death Valley National Monument was selected as a site to study at-satellite estimates of surface reflectance because an undisturbed surface brightness gradient occurs within the boundary of the Monument. Death Valley is a narrow graben partly filled by saline lake sediments, flanked by alluvial fans and remnants of Tertiary volcanic rocks (Hunt and Mabey, 1966). The graben is extremely arid, being characterized by persistent drought and high potential evaporation (Meigs, 1953). The vegetation component of the landscape, comprised primarily of desert shrubs, exists in a delicate balance with soil moisture derived from seeps and springs that originate in the surrounding mountains (Hunt, 1966). Xerophytic plants are found on Quaternary alluvial fans that exhibit an increasing moisture gradient down the fans. Phreatophytic plants are found among some of the saline silt and sand deposits on the valley floor. Soil moisture content of the saline deposits, and the amount and distribution of vegetation, can vary over time and space because of the relative immediate and direct affect of climate on the landscape and vegetation (Wharton *et al.*, 1990).

Seven mapping units were sampled to represent a brightness gradient, age differentiation, and salinity strata (Table 1). The units were characterized by lake sediments (evaporites, saline silts, and sand) and alluvial fans. Sediment units were represented by eroded rock salt (Qhe), flood plain deposits of recent age (Qf), silty rock salt with smooth facies (Qhs), and silty rock salt with rough facies (Qhr). The alluvial fan units were characterized by older (Qg_2) and younger (Qg_3) of the upper Pleistocene fan gravels, and fan gravels (Qg_4) of more recent age.

Mapping units associated with alluvial fans along the east and west sides of Death Valley represent the age differentiation of desert pavement (Qg_2, Qg_3, and Qg_4), while salt crusted and brown silt covered deposits on the valley floor

TABLE 1. DESCRIPTION OF MAPPING UNITS IN DEATH VALLEY NATIONAL MONUMENT, CALIFORNIA.

Units	Unit Description
Qg_2	**Older of the upper Pleistocene fan gravels.** Bouldery deposits in old alluvial fans. Fan form distinct, but much dissected. Surfaces 50 to 75 feet above present washes. Distinct weathering rind on boulders and cobbles and these much disintegrated regardless whether of carbonate, quartzite, or igneous rock; surface strewn with angular blocks, slabs, and flakes. Varnish less distinct than in younger fan gravel. Some layers cemented with caliche. Interwash surfaces form smooth pavement. Vegetation lacking except for xerophytes along washes.
Qg_3	**Younger of the upper Pleistocene fan gravels.** Mostly pebble- to cobble-size gravel. Stones strongly varnished but are firm; many lack weathering rinds. Surfaces of the deposits mostly less than 10 feet above present washes; occur as fans within present washes. Surfaces protected from floods have desert pavement; eroded surfaces are gullied and mantled with recent cobbles and boulders in embankments along edges of gullies. Vegetation is xerophytic.
Qg_4	**Fan gravel of recent age.** Loose gravel in washes and on small fans along large washes. Mostly cobbles and pebbles, well rounded. Not much sand or silt, few boulders except on fans. No desert varnish or weathering rind except in immediate vicinity of reworked older deposits. Flooded only by runoff from cloudbursts. Ground water deep. Vegetation mostly less xerophytic species.
Qf	**Flood plain deposits of sand and silt.** Surfaces on saltpan have extensive salt crusts and are seasonally flooded and without vegetation. Deposits are mostly a few feet higher than present drainage, and are rarely flooded. Vegetation is phreatophytic.
Qhs	**Silty rock salt, smooth facies.** Surface layer is brown silt 2 to 18 inches thick containing sulfate and borate salts; thins panward. Underlain by smooth layer of rock salt 2 to 18 inches thick that thickens panward. At base is silt. Subject to some flooding by runoff originating on this surface. Vegetation lacking.
Qhr	**Silty rock salt, rough facies.** Two to 5 feet thick; capped by brown silty layer 1 to 2 inches thick containing sulfate salts. Surface rough. Elevated and protected against flooding. Vegetation lacking.
Qhe	**Eroded rock salt.** Silty rock salt, 1 to 15 inches thick; overlies silt. Reworked from other chloride zone deposits. Subject to occasional flooding. Vegetation lacking.

represent a salinity stratification (Qhe, Qf, Qhs, and Qhr). Valley floor deposits also exhibit greater moisture content than valley side mapping units so that the affect of moisture absorption in the short-wave infrared wavebands can be assessed on reflectance estimates. Together, all seven units represent a brightness gradient which can be used to compare reflectance estimates over a range of radiometric and topographic conditions.

Methods

A NOAA-10 AVHRR scene and a Landsat TM scene from 19 January 1989 were used to compare at-satellite surface reflectance estimates from the mapping units. The Landsat TM scene was used to compare at-satellite surface reflectance from four mapping units (Qhe, Qf, Qhs, and Qhr) on the valley floor, and to assess the topographic affects on at-satellite surface reflectance from three mapping units on the alluvial fans along the margins of the valley (Qg_2, Qg_3 and Qg_4). The TM and AVHRR scenes were compared to assess the effects of spectral resolution on estimates of at-satellite surface reflectance for one large mapping unit (Qhe) that could be discerned within both scenes.

Atmospheric components for the at-satellite surface reflectance estimates were derived *in situ* at the time of the satellite overpasses using methods described by Jackson and Slater (1986) and Chavez (1989). Global irradiance (G) was collected over the two AVHRR short-wave reflectance wavebands and the six reflective TM wavebands during clear sky conditions at unobstructed sites. Diffuse irradiance was measured immediately afterward by using an occulting disc to block direct sunlight on the radiometer. The relationship between atmospheric transmittance and *in situ* irradiance measurements, corrected for the optical depth of the atmosphere, were found by Equation 4: i.e.,

$$\tau_\lambda = e^{\ln[(G_\lambda - D_\lambda)/BW_\lambda/\cos\theta E_\lambda]/\sec\theta} \quad (4)$$

where

τ is the transmittance coefficient for waveband λ,
θ is the solar zenith angle,
G is the global irradiance integrated over waveband λ,
D is the diffuse irradiance integrated over waveband λ,
BW is the spectral bandwidth of λ, and
E is the top of the atmosphere irradiance in waveband λ.

At-satellite surface reflectance was calculated from the Landsat image for each of the six TM wavebands, the combined red through near infrared waveband (TM3 and TM4), the visible waveband (TM1 through TM3), the visible through near infrared waveband (TM1 through TM4), and over all six reflective TM wavebands together. The average reflectance from each mapping unit was computed for a 3 by 3 sample from the image at the site where each of five *in situ* measurements were taken.

In situ surface reflectance was computed for four sites (Qhe, Qf, Qhs, and Qhr) on the valley floor from spectral reflectance measurements made with a Daedalus SpectraFax field portable spectroradiometer. Five or more samples were taken within each mapping unit for a total of 25 readings per unit. The field data were collected to characterize the average *in situ* reflectance from the mapping units, not to be correlated directly to individual pixels within the satellite observations. *In situ* reflectance was used to validate the average at-satellite surface reflectance for the mapping units using the TM (Figure 1, Table 2) and the AVHRR (Figure 2, Table 3) wavebands. Certainly these highly reflecting surfaces have pronounced non-Lambertian characteristics, so that these field data may not represent the total spectral variation within the units; however, the samples do provide a

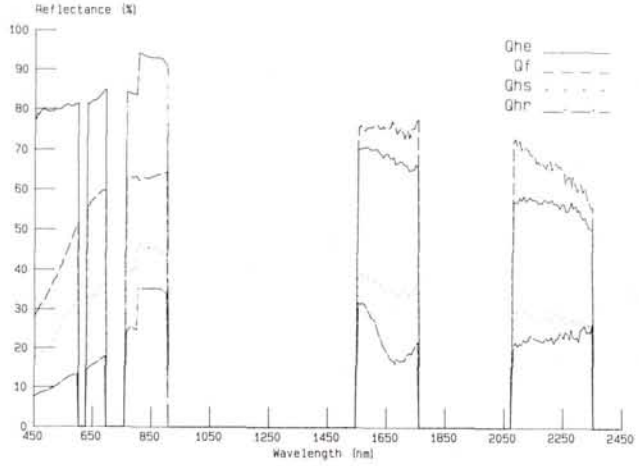

Figure 1. *In situ* reflectance from surficial mapping units in Death Valley National Monument in the Landsat TM wavebands.

measure of the average surface reflectance (Deering *et al.*, 1990). The field samples were only used to evaluate the affect of taking reflectance measurements from different parts of the electromagnetic spectrum. As such, these field data provided some means to validate the results of the at-satellite surface reflectance estimates even though they may not represent the absolute long-term average reflectance of these surfaces.

Results

The primary objective of this research was to examine the sources of variation in at-satellite surface reflectance made from Landsat TM and NOAA's AVHRR because different waveband intervals were involved. However, the large difference in the spatial resolution of the TM (30m) and the AVHRR (1100m) made it difficult, if not impossible, to compare spatially coincident sites for all four mapping units. Therefore, the relatively large eroded rock salt (Qhe) mapping unit was used to compare TM and AVHRR, while the TM reflectance was compared to the in situ reflectance for all four mapping units. The *in situ* measurements were used as a baseline to compare the relative performance of different TM band combinations under the influence of a surface brightness gradient. All field samples were located on the salt and silt encrusted floor of Death Valley so that the influence from topography would be minimized in this analysis, yet the non-Lambertian scattering effects were inherent in the *in situ* reflectance. This was particularly noticeable when the TM and *in situ* reflectance were compared for the rough Qhr surface.

At-Satellite Reflectance Derived from Landsat TM Spectral Wavebands

In general, each of the four saline, salt encrusted mapping units exhibited a wide reflectance range among the individual TM waveband intervals (Table 2). The lowest and highest reflectance always occurred in the TM7 and TM4 wavebands, respectively. For example, reflectance ranged from 0.08 to 0.98 from Qhe, from 0.19 to 0.79 from Qf, from 0.20 to 0.46 from Qhs, and from 0.23 to 0.45 from Qhr. The relatively large difference between the at-satellite surface reflectance and the *in situ* reflectance suggested that no single TM band compared well consistently among all four mapping units.

The four waveband combinations (ρ_{s1}, ρ_{s2}, ρ_{s3}, ρ_{s4}) represented closer agreement between the at-satellite and *in situ* reflectance than any of the individual wavebands, although, the combinations examined in this study resulted in a wide range of at-satellite surface reflectance values (see Table 2). For example, at-satellite surface reflectance ranged from 0.73 to 0.83 from Qhe, 0.52 to 0.64 from Qf, 0.28 to 0.37 from Qhs, and 0.26 to 0.36 from Qhr. The red through near-infrared waveband always showed the highest among these values, while the visible waveband generally showed the lowest reflectance. The absolute difference between the at-satellite surface reflectance and the *in situ* reflectance compared very favorably with all four waveband combinations for the Qhe,

TABLE 2. COMPARISON BETWEEN SURFACE REFLECTANCE DERIVED FROM LANDSAT THEMATIC MAPPER DATA AND *in situ* REFLECTANCE MEASUREMENTS FROM MAPPING UNITS IN DEATH VALLEY NATIONAL MONUMENT.

	Qhe			Qf			Qhs			Qhr			
	ρ_s	ρ_f	Δ	ρ_s	ρ_f	Δ	ρ_s	ρ_f	Δ	ρ_s	ρ_f	Δ	$\Sigma \lvert \Delta \rvert$
ρ_{TM1}	0.76	0.79	0.03	0.52	0.33	0.19	0.27	0.20	0.07	0.23	0.09	0.14	0.29
ρ_{TM2}	0.72	0.81	−0.09	0.51	0.45	0.06	0.27	0.29	−0.02	0.25	0.12	0.13	0.17
ρ_{TM3}	0.68	0.83	−0.15	0.50	0.58	−0.08	0.28	0.34	−0.06	0.27	0.16	0.11	0.29
ρ_{TM4}	0.98	0.90	0.08	0.79	0.63	0.16	0.46	0.43	0.03	0.45	0.31	0.14	0.27
ρ_{TM5}	0.22	0.69	−0.47	0.40	0.75	−0.35	0.28	0.36	−0.08	0.29	0.23	0.06	0.90
ρ_{TM7}	0.08	0.56	−0.48	0.19	0.66	−0.47	0.20	0.28	−0.08	0.23	0.23	0.00	1.03
ρ_{s1}	0.83	0.87	−0.04	0.64	0.61	0.03	0.37	0.38	−0.01	0.36	0.24	0.12	0.08
ρ_{s2}	0.73	0.81	−0.08	0.52	0.48	0.04	0.28	0.29	−0.01	0.26	0.13	0.13	0.13
ρ_{s3}	0.78	0.84	−0.06	0.57	0.54	0.03	0.31	0.34	−0.03	0.29	0.19	0.10	0.12
ρ_{s4}	0.74	0.80	−0.06	0.55	0.56	−0.01	0.31	0.34	−0.03	0.29	0.20	0.09	0.10

ρ_s At-satellite surface reflectance for the specified wavebands and waveband combinations
ρ_f *In situ* reflectance measured over the specified wavebands and waveband combinations with a field radiometer
Δ Difference between at-satellite surface reflectance and *in situ* reflectance for the specified wavebands
ρ_{s1} Red and near-infrared waveband combination (TM3, TM4)
ρ_{s2} Visible waveband interval (TM1, TM2, TM3)
ρ_{s3} Visible and near infrared waveband interval (TM1, TM2, TM3, AND TM4)
ρ_{s4} Surface reflectance (TM1, TM2, TM3, TM4, TM5, AND TM7)
$\Sigma \lvert \Delta \rvert$ Sum of the absolute differences between at-satellite surface reflectance and *in situ* reflectance for the Qhe, Qf, and Qhs mapping units

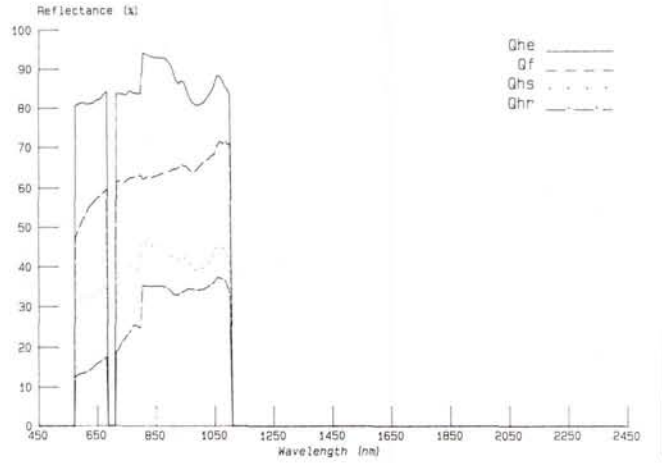

Figure 2. *In situ* reflectance from surficial mapping units in Death Valley National Monument in the NOAA AVHRR wavebands.

Qf, and Qhs mapping units. The lowest overall difference was found in the red through near infrared waveband interval: −0.04 for Qhe, 0.03 for Qf, and −0.01 for Qhs. The Qhr mapping unit showed a large difference between at-satellite surface reflectance and in situ reflectance for all four waveband combinations, due undoubtedly to greater scattering, suggesting that the Qhr *in situ* reflectance was not as reliable as the other *in situ* measurements. However, the remarkably close agreement between the at-satellite surface reflectance and the *in situ* reflectance indicated that Landsat TM could measure surface reflectance from the other three mapping units (Figure 3).

Relationship between Landsat and AVHRR At-satellite Surface Reflectance

At-satellite surface reflectance measurements from the TM and AVHRR wavebands were compared to assess whether similar values could be derived from the two different satellites. At-satellite surface reflectance was compared only for the brightest saltpan deposit (Qhe) because the large spatial resolution of the AVHRR made it difficult to select coincident spatial samples for the other three mapping units. At-satellite surface reflectance for the red (TM3 and AV1) waveband and the near-infrared (TM4 and AV2) waveband were compared to each other and to the *in situ* reflectance from the Qhe mapping unit (Table 3). TM3 and AV1 spectral bandwidths were similar, but not identical, while the AV2 bandwidth was significantly wider than the comparable TM4 bandwidth (see Figures 1 and 2). The behavior of the reflectance curves within the bandwidths, though, appeared to be similar so that a direct comparison was made when the radiance and irradiance were standardized by bandwidth.

The red waveband at-satellite surface reflectance showed considerable difference between TM3 (0.68) and AV1 (0.96); and both values were considerably different from the *in situ* reflectance in those wavebands, 0.83 and 0.82, respectively. Because the TM3 and AV1 wavebands were similar but not identical, the AV1 surface reflectance was compared to the interval over the TM2 and TM3 bands. Little improvement was found by including the extra bandwidth. The near-infrared waveband at-satellite surface reflectance difference was even greater, 0.98 for TM4 and 0.51 for AV1, while both differed considerably from the *in situ* reflectance measurements. The best agreement between the two at-satellite measurements of surface reflectance was found with the visible through near-infrared waveband interval using either TM2, TM3, and TM4 (0.78) or TM3 and TM4 (0.83), and AV1 and AV2 (0.81). Although the waveband intervals were not identical, they were close enough to derive surface reflectance differences of only 0.03 and 0.02, respectively. Both values agreed favorably with the 0.84 *in situ* reflectance in this waveband.

Effect of Topography on At-satellite Surface Reflectance

Topographic effects on spectral reflectance have been a common problem in satellite observations, yet no completely acceptable method for correcting topographic influences has been proposed. The method used in this paper adjusted solar zenith angles to a horizontal surface to solar zenith angles to the topographic surface. Thus, when the land surface was facing into the sun, solar zenith angles could be reduced relative to the surface slope. However, when slopes were facing away from the sun and not receiving direct solar illumination, this model would over correct the reduction in solar zenith angle, resulting in much brighter reflectance than expected.

The difference between at-satellite surface reflectance and at-satellite topographically corrected surface reflectance was evaluated by subtracting the former from the latter. Reflectance difference image values ranged from 0.26 to more than −0.35. Regions of Death Valley that exhibited small differences in reflectance (−5 percent to +5 percent) occurred the most in the study area (85 percent of area); and slopes as low as 0 to 5 degrees resulted in reflectance differences this large. However, slopes between 6 and 10 degrees were necessary to achieve 0.06 to 0.10 difference in reflectance due to topography (Table 4). The practical affect of topography on surface reflectance was assessed by comparing average at-sat-

TABLE 3. COMPARISON BETWEEN LANDSAT TM, NOAA AVHRR, AND *IN SITU* REFLECTANCE FROM ERODED ROCK SALT (QHE) IN DEATH VALLEY NATIONAL MONUMENT

Wavebands	ρ_s	ρ_f	Δ_{sf}
TM3	0.68	0.83	−0.15
AV1	0.96	0.82	0.14
Δ_s	−0.28	0.01	
TM2 and TM3	0.70	0.82	−0.12
AV1	0.96	0.82	0.14
Δ_s	−0.26	0.00	
TM4	0.98	0.90	0.08
AV2	0.51	0.87	−0.36
Δ_s	0.47	0.03	
TM2-TM4	0.78	0.84	−0.06
AV1-AV2	0.81	0.84	−0.03
Δ_s	−0.03	0.00	
TM3-TM4	0.83	0.87	−0.04
AV1-AV2	0.81	0.84	−0.03
Δ_s	0.02	0.03	

ρ_s At-satellite in-band surface reflectance measured over the specific waveband intervals

ρ_f In-band reflectance measured *in situ* with field radiometer over specified waveband intervals

Δ_{sf} Difference between at-satellite surface reflectance and *in situ* reflectance

Δ_s Difference between TM and AVHRR at-satellite surface reflectance

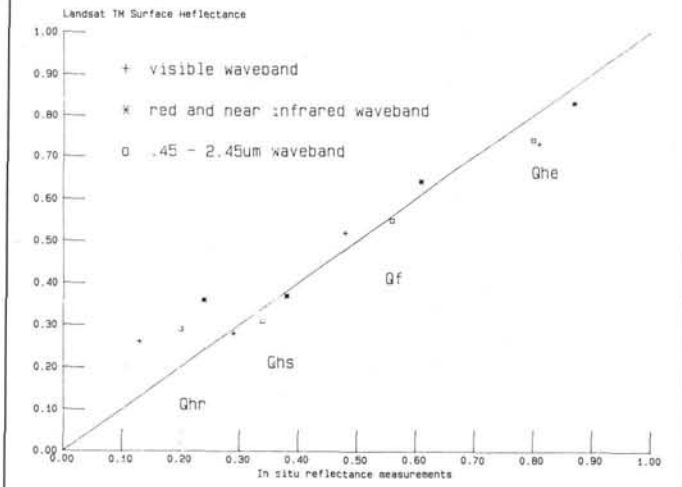

Figure 3. Comparison between at-satellite and *in situ* reflectance from surficial mapping units in Death Valley National Monument.

ellite surface reflectance and topographically corrected at-satellite surface reflectance for three Quaternary fan gravel deposits on both the west and east side of Death Valley National Monument. These surfaces represented sites that varied by slope and aspect so that illumination differences were expressed between samples. Topographically corrected at-satellite surface reflectance was calculated for two waveband intervals: the visible through near-infrared interval, and the visible through short-wave infrared interval. The largest difference between the two surface reflectance estimates at any of the sites was 0.02 (Table 4). The slopes at these sites ranged from 1 to 8 degrees, and slope aspects faced to the northeast or southeast. Under gentle slope conditions, the affect of topography appeared to be insignificant. Larger at-satellite surface reflectance differences were affected more by the waveband interval than by topography under these slope conditions.

Conclusions

Many factors affect the spatial and temporal variability of the Earth's surface reflectance. Most of these factors that are directly related to the terrestrial environment change in a relatively slow and predictable way, such as the natural phenological progression of vegetation through the growing season. Yet some factors are more ephemeral and change abruptly over time and space. These factors are often related to the natural and anthropogenic modifications of the terrestrial landscape, and to the natural variation of climate and the daily sky conditions. Therefore, surface reflectance measurements can be an important indicator of change in the terrestrial landscape; however, it is very difficult to resolve all of the parameters, both terrestrial and atmospheric, that affect at-satellite surface reflectance measurements.

Measurements of surface reflectance from satellites suffer particularly from the abrupt variability of atmospheric conditions. Both atmospheric scattering and transmittance are affected by the amount and distribution of gas molecules and solid particles, and these effects vary throughout the day as a result of changes in both the condition of the atmosphere and the optical air mass. The temporal variability of solid particles in the atmosphere over arid and semiarid landscapes presents an especially formidable problem because the density and vertical distribution of particles in the atmosphere is related to the intensity and direction of surface winds and the type and distribution of terrestrial components in the landscape.

The type and distribution of terrestrial components in arid and semiarid landscapes affect surface reflectance in at least two important ways. Unvegetated landscape units generally exhibit a brightness gradient that is related to the amount of silt and salt deposited on the surface. Reflectance from the salt encrusted surfaces can be so intense that the scattering and transmittance characteristics of the lower atmosphere affect the path, and subsequent amount, of radiation leaving the surface and passing through the atmosphere. The magnitude of this problem is related to surface brightness so that reflectance from darker silt covered deposits is affected less than reflectance from saltpan deposits. The exact relationship between surface brightness and the amount of radiation lost to atmospheric effects is still unresolved; however, awareness of this problem in arid and semiarid landscapes can help to explain differences between *in situ* reflectance measurements and reflectance measurements made at some distance above the ground. The results of this study did not indicate that any conclusive effect of surface brightness was apparent in the at-satellite surface reflectance measurements. At-satellite red through near-infrared surface reflectance from Qhe (0.83), the brightest surface, was 0.04 less than *in situ* reflectance (0.87), while at-satellite red through near-infrared surface reflectance from the next brightest surface, Qf (0.64), was 0.03 higher than *in situ* reflectance (0.61). Then the darker Qhs *in situ* reflectance (0.38) was nearly the same as the at-satellite red through near-infrared surface reflectance (0.37). Because the Qhe at-satellite reflectance values were lower than surface reflectance, it could be that scattering in the lower atmosphere did have some direct impact on reflected radiation; yet these effects were difficult to distinguish from other factors such as the amount and distribution of moisture in the Qhe

TABLE 4. TOPOGRAPHIC AFFECTS ON LANDSAT AT-SATELLITE SURFACE REFLECTANCE FROM QUARTENARY FAN GRAVEL DEPOSITS ON TRAIL CANYON FAN, DEATH VALLEY NATIONAL MONUMENT, CALIFORNIA.

Mapping Unit	ρ_s^1	ρ_t	ρ_s^2	ρ_t	α	β
Qg_2	0.12	0.11	0.15	0.14	6	133
Qg_2	0.13	0.13	0.16	0.16	7	104
Qg_2	0.16	0.16	0.18	0.18	5	65
Qg_2	0.11	0.11	0.14	0.14	5	81
Qg_3	0.10	0.11	0.13	0.13	8	115
Qg_3	0.15	0.15	0.18	0.18	4	80
Qg_3	0.10	0.11	0.12	0.13	7	54
Qg_4	0.11	0.12	0.13	0.14	2	45
Qg_4	0.16	0.16	0.18	0.18	1	15
Qg_4	0.09	0.11	0.11	0.12	7	90
Qg_4	0.15	0.14	0.16	0.15	1	28

ρ_s^1 At-satellite surface reflectance in the red and near infrared waveband
ρ_s^2 At-satellite surface reflectance in the visible through short-wave infrared waveband
ρ_t Topographically corrected at-satellite surface reflectance
α Surface slope in degrees
β Surface aspect in degrees

mapping unit, or *in situ* scattering recorded by the radiometer. The absolute difference between at-satellite and *in situ* surface reflectance was so small that any non-Lambertian scattering or subtle change in the surface reflectance parameters could also have been responsible for these differences.

Secondly, topography affects surface reflectance because terrestrial components receive different amounts of solar illumination depending upon the slope and aspect of the ground and the position of the sun relative to the topographic surface. Some topographic conditions were so severe in the mountain areas surrounding Death Valley National Monument that no solution was available to correct surface reflectance measurements. However, when terrestrial landscape units were exposed to direct solar illumination, the influence of topography on at-satellite surface reflectance was less than expected in this study. Although considerable differences existed between at-satellite surface reflectance and at-satellite topographically corrected surface reflectance for extremely steep slopes, the practical affect of topography on surface reflectance from relatively gentle slopes, e.g., areas not completely blocked from receiving direct solar insolation, were quite small, if not negligible, and well within differences that could have resulted from measurement or rounding errors in the algorithms.

Spectral resolution affected at-satellite and *in situ* surface reflectance measurements more than any other factor in this study. Considerably different surface reflectance measurements were made in the visible, red through near infrared, and the reflective (0.45- to 2.4-μm) waveband intervals, both *in situ* and at-satellite. Yet the close agreement between both the TM and AVHRR at-satellite surface reflectance and the *in situ* reflectance measured over the red through near infrared waveband interval indicated that this waveband would be the best choice to monitor changes in the terrestrial landscape. The results of this study suggested that reliable surface reflectance measurements could be obtained from the TM and AVHRR sensors, thereby providing the means to monitor the temporal and spatial variability of surface reflectance at both the local and regional scale in arid and semiarid environments. Further work is required to confirm that reflectance would be a good indicator of disturbance, and to distinguish between the effects of natural and anthropogenic factors. However, these results have shown that a land quality indicator, such as surface reflectance, is available to correlate with variation in the terrestrial components of arid and semiarid landscapes; and perhaps, in the long-term, surface reflectance may help to identify the nature of the processes responsible for degradation in land quality.

References

Chahine, M. T., D. J. McCleese, P. W. Rosenkranz, and D. H. Staelin, 1983. Interaction mechanisms within the atmosphere, Chapter 5, Volume 1, *Manual of Remote Sensing, Second Edition* (R. N. Colwell, editor), American Society for Photogrammetry and Remote Sensing, Falls, Church, Virginia.

Charney, J. C., W. J. Quirk, S. H. Chow, and J. Kornfield, 1977. A comparative study of the effect of albedo change of drought in semiarid regions, *Journal of the Atmospheric Sciences*, 34:1366-1385.

Chavez, P. S., Jr., 1989. Radiometric calibration of Landsat Thematic Mapper multispectral images, *Photogrammetric Engineering & Remote Sensing*, 55:1285-1294.

Chen, T. S., and G. Ohring, 1984. On the relationship between clear sky planetary albedo and surface albedos, *Journal of the Atmospheric Sciences*, 41:156-158.

Civco, D. L., 1989. Topographic normalization of Landsat Thematic Mapper digital imagery, *Photogrammetric Engineering & Remote Sensing*, 55(9):1303-1309.

Davis, P. A., G. L. Berlin, and P. S. Chavez, Jr., 1987. Discrimination of altered basaltic rocks in the southwestern United States by analysis of Landsat Thematic Mapper data, *Photogrammetric Engineering & Remote Sensing*, 53:45-55.

Deering, D. W., T. F. Eck, and J.Otterman, 1990. Bi-directional reflectances of selected desert surfaces and their three-parameter soil characterization, *Agricultural and Forest Meteorology*, 52:71-93.

Dozier, J., and A. H. Strahler, 1983. Ground investigations in support of remote sensing, *Manual of Remote Sensing*, Second Edition (R. N. Colwell, editor), American Society for Photogrammetry and Remote Sensing, Falls Church, Virginia, pp. 959-986.

Dregne, H. E., 1981. Magnitude and characteristics of desertification of world's arid lands, *Abstracts of Papers of the International Scientific Symposium on Combating Desertification through Integrated Development*, Tashkent, Moscow, UNEPCOM, pp. 21-23.

Frank, T. D., 1984. The effect of change in vegetation cover and erosion patterns on albedo and texture of Landsat images in a semiarid environment, *Annals of the Association of American Geographers*, 74:393-407.

Garnier, B. J., and A. Ohmura, 1968. A method of calculating the direct short-wave radiation income of slopes, *Journal of Applied Meteorology*, 7:796-800.

Gerasimov, I. P., 1986. *Arid Land Development and the Combat against Desertification: An Integrated Approach*, United Nations Environment Programme, USSR Commission for UNEP, 145 p.

Gillespie, A. R., A. B. Kahle, and F. D. Palluconi, 1984. Mapping alluvial fans in Death Valley, California, using multichannel thermal infrared images, *Geophysical Research Letters*, 11: 1153-1156.

Graetz, R., and M. Gentle, 1982. The relationship between reflectance in the Landsat wavebands and the composition of an Australian semiarid shrub rangeland, *Photogrammetric Engineering & Remote Sensing*, 11:1721-1730.

Graetz, R. D., and R. P. Pech, 1988. The assessment and monitoring of sparsely vegetated rangelands using calibrated Landsat data, *Int. Journal of Remote Sensing*, 9:1201-1222.

Hunt, C. B., 1966. *Plant Ecology of Death Valley, California*, U.S. Geological Survey Professional Paper 509, United States Government Printing Office, Washington, D.C., 68 p.

Hunt, C. B., and D. R. Mabey, 1966. *Stratigraphy and Structure Death Valley, California*, U.S. Geological Survey Professional Paper 494-A, United States Government Printing Office, Washington, D.C., 162 p.

Jackson, R. D., and P. N. Slater, 1986. Absolute calibration of field reflectance radiometers, *Photogrammetric Engineering & Remote Sensing*, 52:189-196.

Justice, C. O., J. R. G. Townshend, and B. J. Choudhury, 1989. Comparison of AVHRR and SMMR data for monitoring vegetation phenology on a continental scale, *Int. Journal of Remote Sensing*, 10:1607-1632.

Kaufman, Y. K., 1989. The atmospheric effect on remote sensing and its correction, Chapter 9, in *Theory and Applications of Optical Remote Sensing* (G. Asrar, editor), John Wiley & Sons, New York.

Kawata, Y., S. Ueno, and T. Kusaka, 1988. Radiometric correction for atmospheric and topographic effects on Landsat MSS images, *International Journal of Remote Sensing*, 9:729-748.

McDaneil, K., and R. Haas, 1982. Assessing mesquite-grass vegetation condition from Landsat, *Photogrammetric Engineering & Remote Sensing*, 3:441-450.

Meigs, P., 1953. World distribution of arid and semi-arid homoclimates, *Reviews of Research on Arid Zone Hydrology*, UNESCO, Paris, pp. 203-209.

Nelson, R., D. C. Case, N. Horning, V. Anderson, and S Pillai, 1987.

Continental land cover assessment using Landsat MSS data, *Remote Sensing of Environment*, 21:61-81.

Nunez, M., W. J. Skirving, and N. R. Viney, 1987. A technique for estimating regional surface albedos using geostationary satellite data, *Journal of Climatology*, 7:1-11.

Otterman, J., and C. J. Tucker, 1985. Satellite measurements of surface albedo and temperatures in semi-desert, *Journal of Climate and Applied Meteorology*, 24:228-235.

Pech, R. P., A. W. Davis, R. P. Lamacraft, and R. D. Graetz, 1986. Calibration of Landsat data for sparsely vegetated semi-arid rangelands, *Int. Journal of Remote Sensing*, 7:1729-1750.

Petersen, G. V., K. F. Connors, D. A. Miller, R. L. Day, and T. W. Gardner, 1987. Aircraft and satellite remote sensing of desert soils and landscapes, *Remote Sensing of Environment*, 23:253-271.

Robinove, C., P. S. Chavez, D., Gehring, and R. Holmgren, 1981, Arid land monitoring using Landsat albedo difference images, *Remote Sensing of Environment*, 11:133-156.

Sellers, W. D., 1965. *Physical Climatology*, University of Chicago Press, Chicago, 272 p.

Slater, P. N., 1983. Photographic systems for remote sensing, Chapter 6 in *Manual of Remote Sensing, Second Edition* (R. N. Colwell, editor), American Society for Photogrammetry and Remote Sensing, Falls Church, Virginia, pp. 231-291.

Smith, M. O., S. L. Ustin, J. B. Adams, and A R. Gillespie, 1990a. Vegetation in Deserts I. A regional measure of abundance from multispectral images, *Remote Sensing of Environment*, 31:1-26.

———, 1990b. Vegetation in Deserts II. Environmental influences on regional abundance, *Remote Sensing of Environment*, 31:27-52.

Wharton, R. A., P. E. Wigand, M. R. Rose, R. L. Reinhardt, D A. Mouat, H. E. Klieforth, N. L. Ingraham, J. O. Davis, C. A. Fox, and J. T. Ball, 1990. The North American Great Basin: a sensitive indicator of climatic change, *Plant Biology of the Basin and Range* (C. B. Osmond, L. F. Pitelka, and G. M. Hidy, editors), Ecological Studies Volume 80, Springer-Verlag, New York.

(Received 17 September 1992; revised and accepted 23 March 1993)

Thomas Frank
Thomas Frank is an Associate Professor of Geography and in the Biodiversity Research Program in the Geographic Information Systems Laboratory at the University of Illinois at Urbana-Champaign. Prior to joining the faculty at the University of Illinois in 1979, he received a Ph.D. from the University of Utah, where he concentrated on the application of remote sensing in arid and semi-arid environments. He teaches courses in remote sensing, geographic information systems, and ecological modelling.

Scott Tweddale
Scott Tweddale is the Coordinator of the Geographic Information Systems Laboratory at the University of Illinois where he is responsible for project management and applications support for GIS/image processing research and services. Mr. Tweddale also has an appointment with the U.S. Army Corps of Engineers as a GIS Specialist in the Technical Assistance Center where he supports GIS, remote sensing, and other spatial technologies within the Department of Defense. Mr. Tweddale received both a B.S. and M.S. in geography from the University of Illinois.

David Knapp
David Knapp is employed as a remote sensing specialist at Hughes STX Corporation. Mr. Knapp is responsible for the production of value-added satellite image and GIS data products, especially enhanced image products and digital terrain models from satellite imagery; and maintenance of image processing and GIS software systems at Hughes STX. He has lived in Laurel, Maryland since 1991. He graduated from Pennsylvania State University with a B.S. in geography and then received an M.S. in geography from the University of Illinois.

Win!

Pay your 1995 ASPRS Dues before December 31, 1994 and Win two round trip tickets to and from anywhere in the USA, Frankfurt, Paris or the Caribbean!

Note: The drawing will take place at the end of December, 1994. An award letter will be sent to the winner after the drawing. You can then arrange your trip directly with USAir. Your seat will be reserved (It 's not a standby ticket). Any ticket restrictions must be discussed directly with USAir.

- *DOMESTIC FLIGHTS - USAir only flies within 48 States.*
- *INTERNATIONAL FLIGHTS - USAir only provides you service from within USA to Paris, Frankfurt or the Caribbean.*